

**Ozone monitoring
with the
GOMOS-ENVISAT
experiment version 5**

P. Keckhut et al.

Ozone monitoring with the GOMOS-ENVISAT experiment version 5

**P. Keckhut¹, A. Hauchecorne¹, L. Blano², K. Hocke^{3,4}, S. Godin-Beekmann¹,
J.-L. Bertaux¹, G. Barrot², E. Kyrölä⁵, A. van Gijzel⁶, and A. Pazmino¹**

¹LATMOS-IPSL, CNRS/INSU, UMR 8190, UVSQ, UPMC, Verrières le Buisson, France

²ACRI-ST, Sophia Antipolis, France

³Institute of Applied Physics, University of Bern, Bern, Switzerland

⁴Oeschger Centre for Climate Change Research, University of Bern, Bern, Switzerland

⁵FMI, Helsinki, Finland

⁶RIVM, Bilthoven, The Netherlands

Received: 28 January 2010 – Accepted: 22 March 2010 – Published: 15 June 2010

Correspondence to: P. Keckhut (keckhut@latmos.ipsl.fr)

Published by Copernicus Publications on behalf of the European Geosciences Union.

Title Page

Abstract

Introduction

Conclusions

References

Tables

Figures

⏪

⏩

◀

▶

Back

Close

Full Screen / Esc

Printer-friendly Version

Interactive Discussion

Abstract

The GOMOS ozone profiles derived have been analyzed to evaluate the GOMOS ability to capture the long-term ozone evolution during its expected recovery phase. Version 5 of the GOMOS data has been compared with two of the longest ground-based instruments based on different techniques and already involved with many other previous space instrument validations. Increasing differences reported in 2006 indicate that some of the retrieved profiles are strongly biased. This bad retrieval is probably due to the increasing dark charge of the detectors combined with an inadequate method for its correction. This effect does not induce a continuous bias but is rather exhibiting a bimodal distribution including the correct profiles and the bad retrievals. For long-term analysis it is recommended to filter the data accordingly. The new method of dark charge estimate that is proposed to be implemented in the version 6 of the ESA algorithm, seems to reduce significantly the occurrence of such effects and will allow to monitor stratospheric ozone using GOMOS data with better confidence.

1 Introduction

Since the discovery of the Antarctic ozone hole by Farman et al. (1985) using a ground-based UV spectrometer, instruments onboard satellites provide observations on a global scale. The early ozone measurements from space with the Total Ozone Mapping Spectrometer (TOMS) confirmed the occurrence of seasonal polar ozone decreases, and provide in addition, the horizontal extension of the ozone hole. While the total column is well adapted to monitor the potential increase of the solar UV irradiance, the distribution of the modifications as a function of altitude is crucial to better understand the processes involved and the climate impact of the ozone changes (WMO, 2007). The two longest records of ozone profiles from space are available from two different types of instrument: the Solar Backscatter Ultraviolet (SBUV(/2)) satellite instruments and the Stratospheric Aerosol and Gas Experiment (SAGE I+II).

Ozone monitoring with the GOMOS-ENVISAT experiment version 5

P. Keckhut et al.

Title Page

Abstract

Introduction

Conclusions

References

Tables

Figures

⏪

⏩

◀

▶

Back

Close

Full Screen / Esc

Printer-friendly Version

Interactive Discussion



Ozone monitoring with the GOMOS-ENVISAT experiment version 5

P. Keckhut et al.

Title Page

Abstract

Introduction

Conclusions

References

Tables

Figures

⏪

⏩

◀

▶

Back

Close

Full Screen / Esc

Printer-friendly Version

Interactive Discussion

The SBUV/2 instrument is a scanning double monochromator measuring backscattered solar radiation in 12 discrete wavelength bands ranging from 252.0 to 339.8 nm. The data are available as partial column ozone layers of around 3 km thick. Retrievals are very sensitive to the a priori profile (Bhartia et al., 2004) and successive spectrometers cross-adjustments require comparisons with other data sources (Petrovavlovskikh et al., 2005; Nazaryan and McCormick, 2005; Fioletov et al., 2006; Terao and Logan, 2006) to provide ozone series on a consistent scale using the full sequence of NOAA satellites (Stolarski and Frith, 2006).

The SAGE measurement technique (McCormick et al., 1989) is based on solar occultation, with ozone profile measurements obtained at sunrise and sunset on each of 14 orbits per day. This technique provides relatively high vertical resolution (~ 1 km) and very small long-term drifts resulting from instrument calibration. However, spatial sampling is limited, and it takes approximately one month to sample the latitude range 60° N to 60° S.

Biases between the SAGE II and some SBUV instruments are reported (Nazaryan and McCormick, 2005; Fioletov et al., 2006; Terao and Logan, 2006). These biases, of several percent, are the largest in the upper stratosphere and will contribute to differences in trends derived from SAGE II and SBUV data. However, both series now better converge about long-term trend estimates and show significant declines of around 10–15% (over 17 years) through 1995 when averaged over 60° N– 60° S and altitudes of 35 to 50 km (WMO, 2007) and a decline of up to 10% between 20 and 25 km altitude. These decreases did not continue with the same amplitude in the last decade. Solar occultations provide two different times of measurements at sunset and sunrise that frequently introduce instrumental differences and also atmospheric bias due to ozone photochemical diurnal cycle or indirectly temperature tides.

One alternative method, able to provide both good vertical resolutions and sufficient horizontal sampling can be provided by stellar occultation technique. In March 2002 ESA has launched an environmental satellite called ENVISAT carrying the GOMOS spectrometer (Global Ozone Monitoring by Occultation of Stars). One of the main

advantages of any occultation method is the self calibration process (Bertaux et al., 2004; Kyrölä et al., 2004) and the use of stars allows to increase the suitable number of occultations with time of measurement that is reduced. For all these reasons, GOMOS is a good candidate for long-term ozone 4-D distribution monitoring from space.

5 After a few years of operation, the long-term evolution of the GOMOS version 5 of the data is investigated. Comparisons with ground-based ozone series at mid-latitude have been performed showing that potential bias can exist during the last period when the detector capabilities have decreased.

2 Ozone GOMOS retrieval

10 2.1 Method

The occultation technique was developed several decades ago (Hays and Roble, 1968). It is based on a reference stellar spectrum firstly measured when the star can be seen above the atmosphere. When the line of sight crosses the atmosphere, the light is observed through the atmosphere, and the spectrum is modified by absorption, scattering and refraction. Spectra from 248 to 952 nm are spread over several charge coupled devices (CCD) to cover the full spectrum. The UV domain can be used to retrieve ozone. The detailed layout of the GOMOS instrument is already described (Bertaux et al., 2001, 2010). The main derived quantity is the transmission along the line of sight that is calculated by dividing the star spectra measured outside and through the atmosphere. The main benefit of this method is based on its independence of the instrumental characteristics and the ratio provides a measurement self-calibrated and free of calibration coefficients. The challenge of the pointing system consists in keeping the star image in the center of the slit with a good stability. One of the main characteristics of the star occultation technique concerns the conditions of the measurement that can differ from one occultation to the next. The overall quality of the measurements depends on the signal level and also the contrast of the signal compared with

Ozone monitoring with the GOMOS-ENVISAT experiment version 5

P. Keckhut et al.

Title Page

Abstract

Introduction

Conclusions

References

Tables

Figures



Back

Close

Full Screen / Esc

Printer-friendly Version

Interactive Discussion



**Ozone monitoring
with the
GOMOS-ENVISAT
experiment version 5**

P. Keckhut et al.

[Title Page](#)[Abstract](#)[Introduction](#)[Conclusions](#)[References](#)[Tables](#)[Figures](#)[⏪](#)[⏩](#)[◀](#)[▶](#)[Back](#)[Close](#)[Full Screen / Esc](#)[Printer-friendly Version](#)[Interactive Discussion](#)

the background light. The quality of the measurements is thus depending on different conditions defined by the amount of scattering solar light. Dark conditions provide the lowest noise level and the most accurate measurements. To minimize noise the CCD temperature has been reduced. For ozone, the UV and visible domain, that provide the largest absorption bands, are the most appropriate part of the spectrum. To gain a good spatial coverage a wide variety of stars are used. However, for signal to noise ratio issues, only the 70 brightest stars were selected, as described in Hauchecorne et al. (2005). Some of them provide a strong UV spectrum favorable for ozone absorption retrieval and some of them exhibit a smaller signal. During the ESA-ENVISAT commissioning phase, a large program of coincident ground-based measurements using lidar, ozonsonde, and microwave profilers has been put in place and which is still being continued. All these data permitted to validate the GOMOS v4.02 ozone profiles and evaluate bias for the different conditions. The star temperature and magnitude determine the signal strength of the observed UV spectrum. The hot and bright stars provide the most favourable conditions for ozone retrieval. Because ozone is quite variable, the collocation is always an issue. Meijer et al. (2004) conducted an intensive program of validation using a very large number of coincident measurements mainly from NDACC (Network for the Detection of Atmospheric Composition Changes) and found the best compromise between spatio-temporal differences and the number of profiles to provide an adequate confidence of 800 km and 20 h. When data are partitioned according to the limb illumination conditions, and compared with ground-based measurements, Meijer et al. (2004), found for bright limb conditions, large negative bias of 18–33%. The bias remains when hot stars are used even if it is reduced. Results improve for twilight and even more for dark conditions with bias smaller than 10% and down to 2.5% for some altitude levels. Star magnitude and temperature (related to spectrum shape) seems to be less critical conditions on the data quality of the retrieval. This study highlighted the large influence of the limb background level on the retrieval.

2.2 Noise estimate and evolution

One important step in the GOMOS data processing is the removal of the background light, coming from the solar light scattered by the atmosphere, and the internal noise of the CCD (dark charge) to extract the star signal. In dark limb conditions, the background light is assumed to be negligible. In the GOMOS PRototype code prototype (GOPR) version 6.0, used in the present operational GOMOS-ESA version 5 processing, the CCD dark charge (DC) is estimated using a measurement performed by pointing the GOMOS telescope in a direction without any star in the field of view, called “dark sky area” (DSA), in the sky. On each orbit a dark sky area measurement is planned around the equator and is used to correct all dark limb occultations performed during the same orbit. The noise of a CCD is increasing exponentially with temperature and doubles every 6–8 °C. In order to take into account this temperature effect, the temperature of the CCD is measured. On GOMOS this measurement is made with a digitization step of 0.4 °C, corresponding to a change of about 4% in dark charge. This digitization effect limits the accuracy of the correction to be applied, especially for high CCD noise.

During the GOMOS life the average dark charge of the CCD presented a quasi-linear increase starting from very low values in 2002 as shown in Fig. 1. The main reason for this increase is the appearance of “hot pixels” on the CCD with a definitively increased noise after particle precipitations occurring mainly in the South Atlantic Anomaly. Another reason is the increase of the CCD temperature from –6 to 0 °C between 2002 and 2009. The evolution of the CCD dark charge and CCD temperature can be followed in the GOMOS Monthly Reports available on: <http://earth.esa.int/pcs/envisat/gomos/reports/monthly/>.

Consequently the inaccuracy of the dark charge correction is also increasing proportionally to the dark charge increase and has an increasing effect on the evaluation of the star spectrum particularly in the UV for faint stars. In the example shown in Fig. 2, the estimated background light after dark charge correction in the upper band of the

Ozone monitoring with the GOMOS-ENVISAT experiment version 5

P. Keckhut et al.

Title Page

Abstract

Introduction

Conclusions

References

Tables

Figures



Back

Close

Full Screen / Esc

Printer-friendly Version

Interactive Discussion



5 CCD (top left of the figure) deviates from 0 in the UV (CCD columns 1–500). A value near 0 is expected in dark limb. Similarly the star spectrum (Fig. 2 bottom left) deviates also from 0 in the UV while a value near 0 is expected at the end of the occultation corresponding to a very low tangent altitude. This bad correction of the UV part of the star spectrum may have some effects on the star spectrum estimate and then in the ozone retrieval itself because it is interpreted by the spectral inversion routine as a lack of ozone.

10 In GOCR version 7.0ab an improved analysis in preparation for the next ESA 6 version is used to estimate the dark charge. In addition to the preceding noise analysis using DSA, another step was added to improve the noise residual using the two side CCDs. The UV flux is estimated to be 0 at lower altitude in upper and lower bands of the CCD and the CCD temperature is estimated assuming that the measured signal is equal to the dark charge. After this adjustment, the star spectrum is close to 0 in the UV (Fig. 2 bottom right part of the figure). The impact on the spectrum in the UV domain is very clear in this new version.

2.3 Impact of the noise on ozone retrieval

20 When data are processed with the DSA noise extraction method in GOMOS-ESA v5 data, the level 1b ozone line density profiles show sometimes a strong negative bias with the largest amplitude above 50 km (Fig. 3 left). These bad retrievals occur mainly when noise is large (twilight and bright conditions) and the signal is low. When the level of the star signal is comparable to the noise, an error in the background estimate has a strong impact on the retrieval. The estimated transmission can then be too large or too small. However, negative transmissions are not allowed for physical reasons and so for this reason, the distribution of bias is not symmetric. We suspect that it is due to the incorrect dark charge correction at shortest wavelengths as explained in the previous section. In these cases when the 240–280 nm section of the spectrum is discarded in the retrieval (corresponding pixels are flagged), the retrieved vertical profiles appear to be less biased (Fig. 3 right) while the overall noise of the measurement increases

**Ozone monitoring
with the
GOMOS-ENVISAT
experiment version 5**

P. Keckhut et al.

Title Page

Abstract

Introduction

Conclusions

References

Tables

Figures

⏪

⏩

◀

▶

Back

Close

Full Screen / Esc

Printer-friendly Version

Interactive Discussion



mainly above 70 km because the accuracy of the O₃ retrieval is mainly driven by the low UV part.

While the reduced spectral range eliminated most of the biased profiles, it increases the noise in the upper part of the ozone profile where ozone variability can be monitored too much (Fig. 3b). The method of improving the ozone retrieval by reducing the spectral window in the UV domain systematically is a strong limitation because not all star occultations were exhibiting biased ozone profiles. As confirmed in the next section, the bias is not distributed uniformly but rather large biases are reported for some conditions. Those bad retrievals can be visually identified as bad retrievals and removed manually from data series for any inter-annual or climatologic studies. Kyrölä et al. (2006) have identified a black list of some stars (18 out of 70) that appear to be suspicious because they provide some bad ozone retrieval while other seem to be more reliable. A new alternative GOPR V7.0ab processing including both the DSA background noise estimates and the new baseline noise correction, described in Sect. 2.2, has been proposed for inclusion in the systematic new ozone GOMOS processing. As shown in Sect. 2.2 the impact on the Dark Charge estimate in the UV range is quite important and improves the star spectrum. The retrieval with such a new correction show that biased ozone profiles are eliminated for occultations done under “bad conditions” and that the quality of occultations with high signal that were unbiased with the GOPR V6.0cf algorithm are processed exhibiting similar results (Fig. 4).

3 Data comparisons

Version 5 of the ESA-GOMOS ozone data have been compared with two long data sets that have been compared with numerous other data sets. Two different techniques are used: lidar and microwaves. The GOMOS data selection was performed in a space box of $\pm 10^\circ$ in latitude and $\pm 20^\circ$ longitude. The brightest stars have been selected which correspond to the stars with an ID from 1 to 70.

Ozone monitoring with the GOMOS-ENVISAT experiment version 5

P. Keckhut et al.

Title Page

Abstract

Introduction

Conclusions

References

Tables

Figures



Back

Close

Full Screen / Esc

Printer-friendly Version

Interactive Discussion



In the framework of the Network of Detection of Atmospheric Composition Changes (Kurylo and Salomon, 1990), some instruments providing ozone profiles are and have been running systematically over decades. Many satellite experiment validations and long-term investigations were performed giving large confidences and those instruments have participated in regular cross-validation exercises (Keckhut et al., 2004). While mid-latitude regions exhibit the best compromise for comparisons in providing the best and largest amount of collocations for dark conditions, the complementary lidar and microwave instruments from the Alpine stations have been used for comparisons with GOMOS profiles on a long-term basis.

3.1 Comparison with Bern microwave

The ground-based microwave radiometer GROMOS is located at Bern (46°57' N, 7°26' E) in Switzerland and observes the middle atmosphere at an elevation angle of 40° in north-east direction (Peter, 1997). GROMOS measures the vertical ozone distribution from 20 to 70 km altitude under almost all weather conditions during day and night since 1994. The instrument is a triple switched 142.175 GHz total power radiometer and contributes primary data to NDACC. The continuous time series of ozone profiles from GROMOS are regularly used for satellite validations and ozone trend studies (Steinbrecht et al., 2009; Dumitru et al., 2006).

The intercomparison of ozone profiles from ENVISAT/GOMOS and GROMOS is similarly performed as the intercomparison of ozone profiles from ENVISAT/GOMOS and the ground-based microwave radiometer SOMORA at Payerne which was described by Hocke et al. (2007). The high-resolution ozone profiles of ENVISAT/GOMOS are adjusted by averaging kernel smoothing to the vertical resolution (about 10 km) of GROMOS. The coincident profile pairs of ENVISAT/GOMOS and GROMOS have a time difference $\Delta t < 1$ h and a horizontal distance of the sounding volumes $d < 800$ km. The relative difference profile of ozone concentration from ENVISAT/GOMOS and GROMOS is given by:

Ozone monitoring with the GOMOS-ENVISAT experiment version 5

P. Keckhut et al.

Title Page

Abstract

Introduction

Conclusions

References

Tables

Figures

⏪

⏩

◀

▶

Back

Close

Full Screen / Esc

Printer-friendly Version

Interactive Discussion



$$\Delta O_3 = [O_3(\text{ENVISAT}) - O_3(\text{GROMOS})]/O_3(\text{GROMOS}). \quad (1)$$

Figure 5 shows the time series of ΔO_3 at altitudes $h=$ 26, 31, 36, 41, 46, and 51 km for the time interval 2002 to 2006. The number n of coincident profile pairs (blue dots) is between 778 and 784 as denoted in the title of the viewgraphs of Fig. 5. The mean biases are ranging between -0.1% and 10.9% . The best agreement is achieved at altitudes from 36 to 41 km. The running mean shows a gradual increase of ENVISAT/GOMOS differences with too small amounts of ozone due to some individual differences of 100% that occur more frequently more obvious in the stratopause region (lower panels of Fig. 5). In 2006, positive biases (20%) are reported at 26 km, a smaller bias over the 31–41 km range, and a larger negative bias over the 46–51 km range (20%). The comparisons reveal that the biases are not systematic but are partitioned in two classes of profiles with one fully unreliable. This conducts to a bimodal distribution of the differences with increasing occurrence of biased profiles. The class of GOMOS profiles presenting a large negative difference with GROMOS microwave data is clearly related with the class of profiles with a strong negative bias shown in Fig. 3.

3.2 Comparisons with the OHP lidar

The ozone lidar measurements are performed using the DIAL method, which requires the emission of two laser wavelengths with different ozone absorption cross-sections. Range resolved measurements are obtained with the use of pulsed lasers. The spectral range of the laser beams is chosen in the ultraviolet where the ozone absorption is most efficient. In the case of the OHP lidar, the absorbed radiation is emitted by a XeCl excimer laser at 308 nm and the reference line is provided by the third harmonic of a Nd:Yag laser at 355 nm (Godin et al., 1989). The reception system includes 4 telescopes of 50 cm diameter with optical fibres mounted in the focal plane in order to collect the laser light and a spectrometer to separate the various detected wavelengths. Photon-counting is used for the acquisition of the lidar signals. The large dynamic of the

Ozone monitoring with the GOMOS-ENVISAT experiment version 5

P. Keckhut et al.

[Title Page](#)[Abstract](#)[Introduction](#)[Conclusions](#)[References](#)[Tables](#)[Figures](#)[⏪](#)[⏩](#)[◀](#)[▶](#)[Back](#)[Close](#)[Full Screen / Esc](#)[Printer-friendly Version](#)[Interactive Discussion](#)

signals is handled by separating each return signal into a low and a high-energy channel for the measurement of ozone in the low and middle-high stratosphere respectively. The ozone number density is computed from the differentiation of the signals. Two additional wavelengths corresponding to the first Stokes vibrational Raman scattering by atmospheric nitrogen of the laser beams are detected in order to retrieve ozone in case of high aerosol loading, (McGee et al., 1993). The lidar measurements are performed during the night and typically last several hours, which results in a spatial resolution of about 100 km, depending on atmospheric conditions. The vertical resolution has to be reduced as a function of altitude due to the decreasing signal-to-noise ratio. It ranges from several hundreds of meters in the lower range to several kilometers above 40 km. The total accuracy ranges from about a few percent below 20 km to more than 10% above 45 km (Godin-Beekmann et al., 2003). The lidar in the present configuration has been operated routinely at OHP since 1994. First stratospheric ozone lidar measurements were performed with a simpler system at OHP in campaign mode in 1985 and 1986. Routine measurements were obtained with the simpler system from 1986 to 1993. The OHP ozone data have been compared to various satellite measurements such as SAGE II, MLS-UARS, GOME, GOMOS, MIPAS, SCIAMACHY (Meijer et al., 2004; Brinksma et al., 2006; Meijer et al., 2006; Cortesi et al., 2007; Iapaolo et al., 2007, Jiang et al., 2007; Rozanov et al., 2007; van Gijsel, 2009).

Comparisons between lidar and GOMOS ozone profiles have been performed with the similar methodology described previously and exhibit a variability of nearly $\pm 20\%$. A clear negative bias in 2006 of 10–20% is observed in most profiles 40 km and less evident at 20 km. The bias profiles correspond mainly to the noisier spectra obtained during twilight and bright conditions.

**Ozone monitoring
with the
GOMOS-ENVISAT
experiment version 5**

P. Keckhut et al.

Title Page

Abstract

Introduction

Conclusions

References

Tables

Figures



Back

Close

Full Screen / Esc

Printer-friendly Version

Interactive Discussion



4 Conclusions

Biases are detected in GOMOS ozone ESA-V5 (corresponding to GOPR6.0cf) data when compared to the ground-based validated NDACC lidar at OHP and the microwave profiles operated at the Alpine station in the northern mid-latitude. While the first years of operation seem to reveal a good agreement between the ground-based and GOMOS measurements, some large biases (10–20%) are observed in 2006 and after. If these biases profiles exist for a wide range of latitude, long-term trend studies with the GOMOS data presently available will be less reliable. These differences are due to some bad retrieval cases corresponding to some star occultations exhibiting weak signals or large noise levels. These biases may be due to an imperfect dark charge correction of the CCD coupled with the regular dark charge increase. The distribution of ozone profiles exhibits a clear bimodal structure that allows a straightforward detection of bad retrievals. Resulting biases in the ozone series do not allow long-term ozone change estimated with the GOMOS-ESA V5 retrieval dataset if disregarding the data quality. One possibility to deal with this consists in removing bad retrievals or some occultations of some known dangerous stars. However, this will reduce the number of measurements.

A new dark charge correction algorithm has been implanted in GOPR V7.0ab. The preliminary comparisons with a subset of data show that the retrieval greatly improves the quality of GOMOS ozone profiles. The full comparison of this data version with a larger set of NDACC validation instruments will be done after the ESA V6 reprocessing with this new algorithm, which should take place in 2010. This work also pointed out the importance of long-term validation of satellite data with ground-based network as provide by NDACC.

Acknowledgements. This work was performed under the framework of the European Integrated Project Geomon selected by the 6th Framework Program (contract number FOP6-2005-Global-4-036677) and by the MeteoSwiss project MIMAH. The French team was supported for ENVISAT validation by the French National Space Agency CNES (Centre National d'Etudes Spatiales). Ground-based data used in this publication were obtained as part of the Network of

Ozone monitoring with the GOMOS-ENVISAT experiment version 5

P. Keckhut et al.

Title Page

Abstract

Introduction

Conclusions

References

Tables

Figures



Back

Close

Full Screen / Esc

Printer-friendly Version

Interactive Discussion



the Detection of the Atmospheric Composition Changes (NDACC) and are publicly available through the NDACC/NOAA web site (<http://www.ndsc.ncep.noaa.gov>) and through the French ETHER web site (<http://ether.ipsl.jussieu.fr/etherTypo/?id=1145>). Lidar data were also supported by the European Space Agency (ESA) through the Envisat Quality Assessment with Lidar ESA project (EQUAL), dedicated to the long-term validation of ozone and temperature profile data from all three atmospheric-chemistry instruments (GOMOS, MIPAS and SCIAMACHY) carried on Envisat, and its follow-up the “Validation with lidar” project (VALID) with a multi-mission focus and extension with the validation of aerosol and cloud properties.



The publication of this article is financed by CNRS-INSU.

References

- Bertaux, J. L., Chipperfeld, M., Dalaudier, F., Fussen, D., Hauchecorne, A., Kyrölä, E., Leppelmeier, G., and Roscoe, H. K.: Envisat GOMOS, An Instrument for Global Atmospheric Ozone Monitoring, coordinated by Readings, C. J. and Wehr, T., ESA SP-1244, 2001.
- Bertaux, J.-L., Hauchecorne, A., Dalaudier, F., Cot, C., Kyrölä, E., Fussen, D., Tamminen, J., Leppelmeier, G.-W., Sofieva, V., Hassinen, S., Fanton d'Andon, O., Barrot, G., Mangin, A., Théodore, B., Guirlet, M., Korablev, O., Snoeij, P., Koopman, R., and Fraisse, R.: First results on GOMOS/ENVISAT, *Adv. Space Res.*, 33(7), 1029–1035, 2004.
- Bertaux, J. L., Kyrölä, E., Fussen, D., Hauchecorne, A., Dalaudier, F., Sofieva, V., Tamminen, J., Vanhellemont, F., Fanton d'Andon, O., Barrot, G., Mangin, A., Blanot, L., Lebrun, J. C., Pérot, K., Fehr, T., Saavedra, L., and Fraisse, R.: Global ozone monitoring by occultation of stars: an overview of GOMOS measurements on ENVISAT, *Atmos. Chem. Phys. Discuss.*, 10, 9917–10076, doi:10.5194/acpd-10-9917-2010, 2010.

Ozone monitoring with the GOMOS-ENVISAT experiment version 5

P. Keckhut et al.

Title Page

Abstract

Introduction

Conclusions

References

Tables

Figures



Back

Close

Full Screen / Esc

Printer-friendly Version

Interactive Discussion



Ozone monitoring with the GOMOS-ENVISAT experiment version 5

P. Keckhut et al.

[Title Page](#)
[Abstract](#)
[Introduction](#)
[Conclusions](#)
[References](#)
[Tables](#)
[Figures](#)




[Back](#)
[Close](#)
[Full Screen / Esc](#)
[Printer-friendly Version](#)
[Interactive Discussion](#)

- Bhartia, P., Wellemeyer, K., Taylor, C., Nath, S. L., and Gopalan, A.: Solar Backscatter Ultraviolet (SBUV) version 8 profile algorithm, in: Proceedings of the Quadrennial Ozone Symposium, 2004, edited by: Zerefos, C., Int. Ozone Comm., Athens, Greece, 295–296, 2004.
- Brinksma, E. J., Bracher, A., Lolkema, D. E., Segers, A. J., Boyd, I. S., Bramstedt, K., Claude, H., Godin-Beekmann, S., Hansen, G., Kopp, G., Leblanc, T., McDermid, I. S., Meijer, Y. J., Nakane, H., Parrish, A., von Savigny, C., Stebel, K., Swart, D. P. J., Taha, G., and Piters, A. J. M.: Geophysical validation of SCIAMACHY Limb Ozone Profiles, *Atmos. Chem. Phys.*, 6, 197–209, doi:10.5194/acp-6-197-2006, 2006.
- Cortesi, U., Lambert, J. C., De Clercq, C., Bianchini, G., Blumenstock, T., Bracher, A., Castelli, E., Catoire, V., Chance, K. V., De Mazière, M., Demoulin, P., Godin-Beekmann, S., Jones, N., Jucks, K., Keim, C., Kerzenmacher, T., Kuellmann, H., Kuttippurath, J., Iarlori, M., Liu, G. Y., Liu, Y., McDermid, I. S., Meijer, Y. J., Mencaraglia, F., Mikuteit, S., Oelhaf, H., Piccolo, C., Pirre, M., Raspollini, P., Ravegnani, F., Reburn, W. J., Redaelli, G., Remedios, J. J., Sembhi, H., Smale, D., Steck, T., Taddei, A., Varotsos, C., Vigouroux, C., Waterfall, A., Wetzell, G., and Wood, S.: Geophysical validation of MIPAS-ENVISAT operational ozone data, *Atmos. Chem. Phys.*, 7, 4807–4867, doi:10.5194/acp-7-4807-2007, 2007.
- Dumitru, D., Hocke, C. K., Kämpfer, N., and Calisesi, Y.: Comparison and validation studies related to ground-base microwave observations of ozone in the stratosphere and mesosphere, *J. Atmos. Sol.-Terr. Phy.*, 68(7), 745–756, 2006.
- Dupuy, E., Walker, K. A., Kar, J., Boone, C. D., McElroy, C. T., Bernath, P. F., Drummond, J. R., Skelton, R., McLeod, S. D., Hughes, R. C., Nowlan, C. R., Dufour, D. G., Zou, J., Nichitiu, F., Strong, K., Baron, P., Bevilacqua, R. M., Blumenstock, T., Bodeker, G. E., Borsdorff, T., Bourassa, A. E., Bovensmann, H., Boyd, I. S., Bracher, A., Brogniez, C., Burrows, J. P., Catoire, V., Ceccherini, S., Chabrillat, S., Christensen, T., Coffey, M. T., Cortesi, U., Davies, J., De Clercq, C., Degenstein, D. A., De Mazière, M., Demoulin, P., Dodion, J., Firanski, B., Fischer, H., Forbes, G., Froidevaux, L., Fussen, D., Gerard, P., Godin-Beekmann, S., Goutail, F., Granville, J., Griffith, D., Haley, C. S., Hannigan, J. W., Höpfner, M., Jin, J. J., Jones, A., Jones, N. B., Jucks, K., Kagawa, A., Kasai, Y., Kerzenmacher, T. E., Kleinböhl, A., Klekociuk, A. R., Kramer, I., Küllmann, H., Kuttippurath, J., Kyrölä, E., Lambert, J.-C., Livesey, N. J., Llewellyn, E. J., Lloyd, N. D., Mahieu, E., Manney, G. L., Marshall, B. T., McConnell, J. C., McCormick, M. P., McDermid, I. S., McHugh, M., McLinden, C. A., Melqvist, J., Mizutani, K., Murayama, Y., Murtagh, D. P., Oelhaf, H., Parrish, A., Petelina, S. V., Piccolo, C., Pommereau, J.-P., Randall, C. E., Robert, C., Roth, C., Schneider, M., Senten,

Ozone monitoring with the GOMOS-ENVISAT experiment version 5

P. Keckhut et al.

[Title Page](#)
[Abstract](#)
[Introduction](#)
[Conclusions](#)
[References](#)
[Tables](#)
[Figures](#)




[Back](#)
[Close](#)
[Full Screen / Esc](#)
[Printer-friendly Version](#)
[Interactive Discussion](#)


C., Steck, T., Strandberg, A., Strawbridge, K. B., Sussmann, R., Swart, D. P. J., Tarasick, D. W., Taylor, J. R., Tétard, C., Thomason, L. W., Thompson, A. M., Tully, M. B., Urban, J., Vanhellemont, F., Vigouroux, C., von Clarmann, T., von der Gathen, P., von Savigny, C., Waters, J. W., Witte, J. C., Wolff, M., and Zawodny, J. M.: Validation of ozone measurements from the Atmospheric Chemistry Experiment (ACE), *Atmos. Chem. Phys.*, 9, 287–343, doi:10.5194/acp-9-287-2009, 2009.

Farman, J. C. and Shanklin, J. D.: Large losses of total ozone in Antarctica reveal seasonal ClO_x/NO_x interaction, *Nature*, 315, 207–210, 1985.

Fioletov, V. E., Tarasick, D. W., and Petropavlovskikh, I.: Estimating ozone variability and instrument uncertainties from SBUV(/2), ozonesonde, Umkehr, and SAGE II measurements: Shortterm variations, *J. Geophys. Res.*, 111, D02305, doi:10.1029/2005JD006340, 2006.

Godin, S., Mégie, G., and Pelon, P.: Systematic Lidar Measurements of the Stratospheric Ozone vertical Distribution, *Geophys. Res. Lett.*, 16(16), 547–550, 1989.

Godin-Beekmann, S., Porteneuve, J., and Garnier, A.: Systematic DIAL ozone measurements at Observatoire de Haute-Provence, *J. Environ. Monitor.*, 5, 57–67, 2003.

Hauchecorne, A., Bertaux, J.-L., Dalaudier, F., Cot, C., Lebrun, J.-C., Bekki, S., Marchand, M., Kyrölä, E., Tamminen, J., Sofieva, V., Fussen, D., Vanhellemont, F., Fanton d'Andon, O., Barrot, G., Mangin, A., Théodore, B., Guirlet, M., Snoeij, P., Koopman, R., Saavedra de Miguel, L., Fraise, R., Renard, J.-B.: GOMOS NO_2 NO_3 : First simultaneous global climatologies of night-time stratospheric NO_2 and NO_3 observed by GOMOS/ENVISAT in 2003, *J. Geophys. Res.*, 110, D18301, doi:10.1029/2004JD005711, 2005.

Hays, P. B. and Roble, R. G.: Stellar spectra and atmospheric composition, *J. Atmos. Sci.*, 25, 1141, 1968.

Hocke, K., Kämpfer, N., Ruffieux, D., Froidevaux, L., Parrish, A., Boyd, I., von Clarmann, T., Steck, T., Timofeyev, Y. M., Polyakov, A. V., and Kyrölä, E.: Comparison and synergy of stratospheric ozone measurements by satellite limb sounders and the ground-based microwave radiometer SOMORA, *Atmos. Chem. Phys.*, 7, 4117–4131, doi:10.5194/acp-7-4117-2007, 2007.

Iapaolo, M., Godin-Beekmann, S., Del Frate, S., Casadio, F., McDermid, S., Leblanc, T., Swart, D., Meijer, Y., Hansen, G., and Stebel, K.: Gome Ozone Profiles Retrieved By Neural Network Techniques: A Global Validation With Lidar Measurements, *J. Quant. Spectrosc. Ra.*, 107, 105–119, doi:10.1016/j.jqsrt.2007.02.015, 2007.

Ozone monitoring with the GOMOS-ENVISAT experiment version 5

P. Keckhut et al.

Title Page

Abstract

Introduction

Conclusions

References

Tables

Figures

⏪

⏩

◀

▶

Back

Close

Full Screen / Esc

Printer-friendly Version

Interactive Discussion



- Jiang, Y. B., Froidevaux, L., Lambert, A., et al.: Validation of Aura Microwave Limb Sounder Ozone by ozonesonde and lidar measurements, *J. Geophys. Res.*, 112, D24S34, doi:10.1029/2007JD008776, 2007.
- Keckhut, P., McDermid, S., Swart, D., McGee, T., Godin-Beekmann, S., Adriani, A., Barnes, J., Baray, J.-L., Bencherif, H., Claude, H., Fiocco, G., Hansen, G., Hauchecorne, A., Leblanc, T., Lee, C. H., Pal, S., Megie, G., Nakane, H., Neuber, R., Steinbrecht, W., and Thayer, J.: Review of ozone and temperature lidar validations performed within the framework of the network for the detection of stratospheric change, *J. Environ. Monitor.*, 6, 721–733, 2004.
- Kurylo, M. J. and Solomon, S.: Network for the Detection of Stratospheric Change, NASA Rep, Code EEU, 1990.
- Kyrölä, E., Tamminen, J., Leppelmeier, G. W., et al.: GOMOS on Envisat: An overview, *Adv. Space Res.*, 33, 1020–1028, 2004.
- Kyrölä, E., Tamminen, J., Leppelmeier, G. W., Sofieva, V., Hassinen, S., Seppälä, A., Verronen, P. T., Bertaux, J.-L., Hauchecorne, A., Dalaudier, F., Fussen, D., Vanhellefont, F. Fanton d'Andon, O. F., Barrot, G., Mangin, A., Theodore, B., Guirlet, M., Koopman, R., Saavedra, L., Snoeij, P., and Fehr, T.: Nighttime ozone profiles in the stratosphere and mesosphere by the Global Ozone Monitoring by Occultation of Stars on Envisat, *J. Geophys. Res.*, 111, D24306, doi:10.1029/2006JD007193, 2006.
- McCormick, M. P., Zawodny, J. M., Veiga, R. E., Larsen, J. C., and Wang, P.-H.: An Overview of SAGE I and II Ozone Measurements, *Planet. Space Sci.*, 37(12), 1567–1586, 1989.
- McGee, T. J., Gross, M., Ferrare, R., Heaps, W. S., and Singh, U. N.: Raman DIAL measurements of Stratospheric Ozone in the presence of volcanic aerosols, *Geophys. Res. Lett.*, 20, 955–958, 1993.
- Meijer, Y. J., Swart, D. P. J., Allaar, M., et al.: Pole-to-pole validation of Envisat GOMOS ozone profiles using data from ground-based and balloon sonde measurements, *J. Geophys. Res.*, 109, D23305, doi:10.1029/2004JD004834, 2004.
- Meijer, Y. J., Swart, D. P. J., Baier, F., et al.: Evaluation of GOME ozone profiles from nine different algorithms, *J. Geophys. Res.*, 111, D21306, doi:10.1029/2005JD006778, 2006.
- Nardi, B., Barnett, J. J., Randall, C. E., et al.: Initial validation of ozone measurements from the High Resolution Dynamics Limb Sounder, *J. Geophys. Res.*, 113, D16S36, doi:10.1029/2007JD008837, 2008.

Ozone monitoring with the GOMOS-ENVISAT experiment version 5

P. Keckhut et al.

Title Page

Abstract

Introduction

Conclusions

References

Tables

Figures

⏪

⏩

◀

▶

Back

Close

Full Screen / Esc

Printer-friendly Version

Interactive Discussion



Nazaryan, H. and McCormick, M. P.: Comparisons of Stratospheric Aerosol and Gas Experiment (SAGE II) and Solar Backscatter Ultraviolet Instrument (SBUV/2) ozone profiles and trend estimates, *J. Geophys. Res.*, 110, D17302, doi:10.1029/2004JD005483, 2005.

Peter, R.: The Ground-based Millimeter-wave Ozone Spectrometer – GROMOS, IAP Research Report, No. 1997-13, Institut für angewandte Physik, Universität Bern, 1997.

Petropavlovskikh, I., Bhartia, P. K., and DeLuisi, J.: New Umkehr ozone profile retrieval algorithm optimized for climatological studies, *Geophys. Res. Lett.*, 32, L16808, doi:10.1029/2005GL023323, 2005.

Rozanov, A., Eichmann, K.-U., von Savigny, C., Bovensmann, H., Burrows, J. P., von Bergen, A., Doicu, A., Hilgers, S., Godin-Beekmann, S., Leblanc, T., and McDermid, I. S.: Comparison of the inversion algorithms applied to the ozone vertical profile retrieval from SCIAMACHY limb measurements, *Atmos. Chem. Phys.*, 7, 4763–4779, doi:10.5194/acp-7-4763-2007, 2007.

Steinbrecht, W., Claude, H., Schonenborn, F., et al.: Ozone and temperature trends in the upper stratosphere at five stations of the Network for the Detection of Atmospheric Composition Change, *Int. J. Remote Sens.*, 30, 3875–3886, 2009.

Stolarski, R. S. and Frith, S. M.: Search for evidence of trend slow-down in the long-term TOMS/SBUV total ozone data record: the importance of instrument drift uncertainty, *Atmos. Chem. Phys.*, 6, 4057–4065, doi:10.5194/acp-6-4057-2006, 2006.

Terao, Y. A. and Logan, J. A.: Effect of Lower Stratospheric Ozone on Trends and Interannual Variability in Tropospheric Ozone, AGU Fall Meeting, 11–15 December 2005, San Francisco, USA, 2006.

Van Gijsel, J. A. E., Swart, D. P. J., Baray, J.-L., Claude, H., Fehr, T., Von Der Gathen, P., Godin-Beekmann, S., Hansen, G. H., Leblanc, T., McDermid, I. S., Meijer, Y. J., Nakane, H., Quel, E. J., Steinbrecht, W., Strawbridge, K. B., Tatarov, B., and Wolfram, E. A.: Global validation of ENVISAT ozone profiles using lidar measurements, *Int. J. Remote Sens.*, 30, 3987–3994, doi:10.1080/01431160902821825, 2009.

WMO (World Meteorological Organization): Scientific Assessment of Ozone Depletion: 2006, Global Ozone Research and Monitoring Project – Report No. 50, Geneva, 572 pp., 2007.

Ozone monitoring with the GOMOS-ENVISAT experiment version 5

P. Keckhut et al.

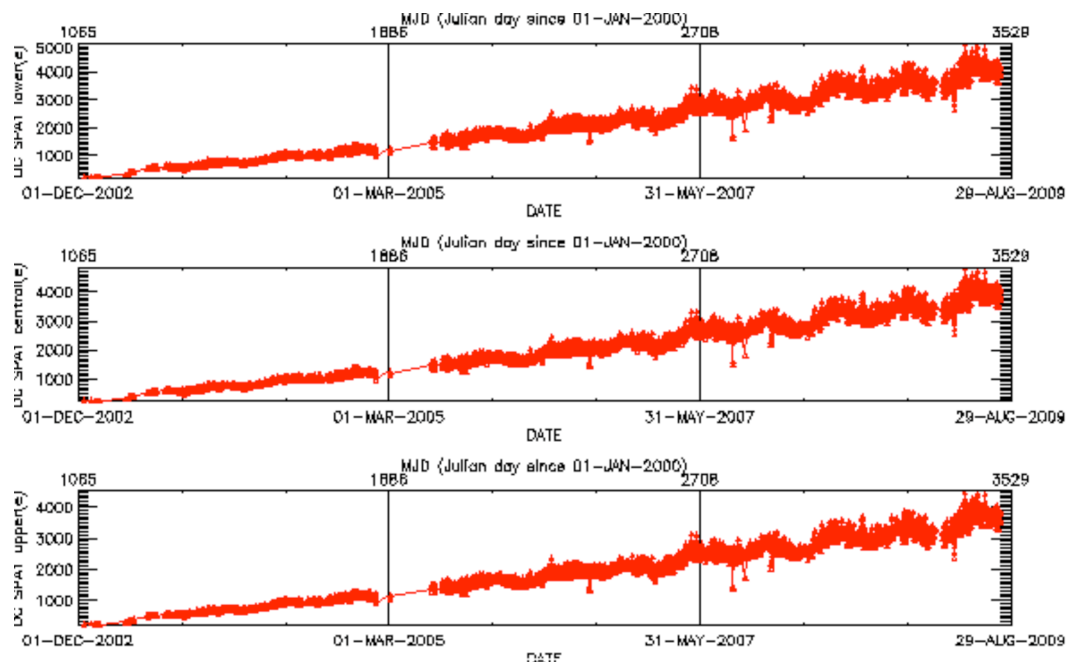


Fig. 1. Dark charge time evolution given by the central band of the CCD (middle) used to acquire star signal and the two other bands of the same CCD in the upper and lower side dedicated to limb background estimate. Here signal corresponds to calibration mode when instrument is not pointing at any star called “dark sky area”.

[Title Page](#)
[Abstract](#)
[Introduction](#)
[Conclusions](#)
[References](#)
[Tables](#)
[Figures](#)
[⏪](#)
[⏩](#)
[◀](#)
[▶](#)
[Back](#)
[Close](#)
[Full Screen / Esc](#)
[Printer-friendly Version](#)
[Interactive Discussion](#)

Ozone monitoring with the GOMOS-ENVISAT experiment version 5

P. Keckhut et al.

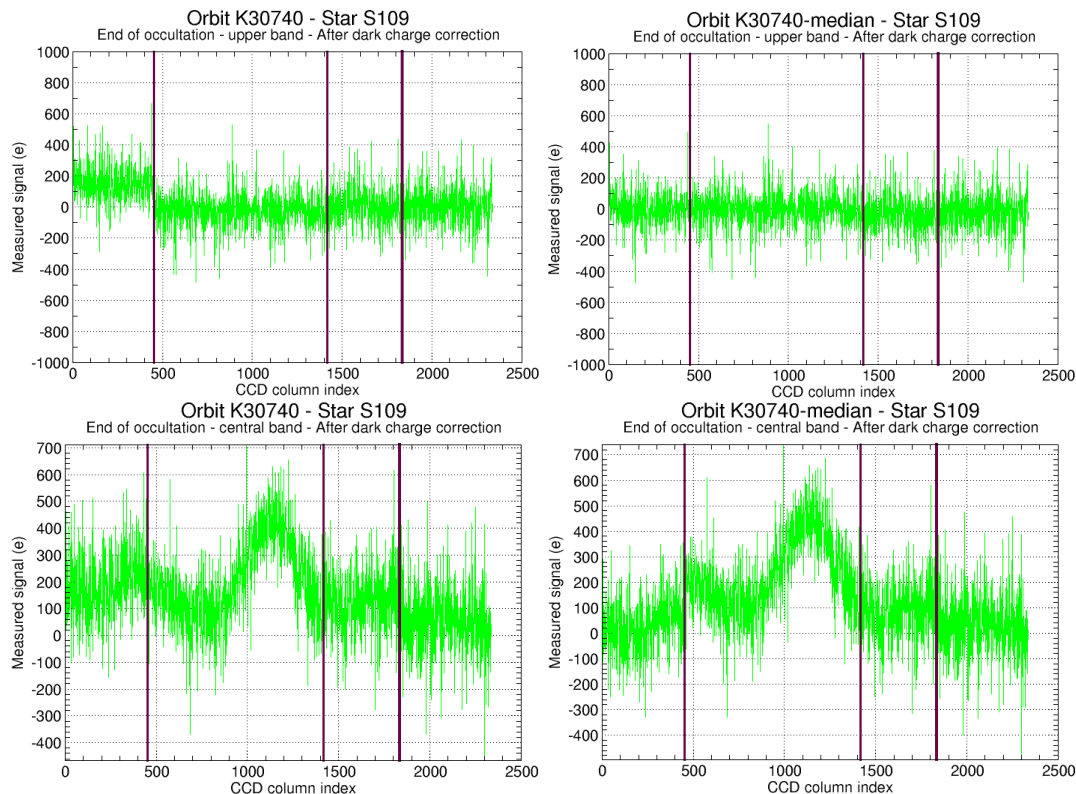


Fig. 2. Dark charge bias correction using two methods and the respective star spectrum with noise extraction. Noise estimated for “Dark Sky Area” method V6.0cf (top left). Example of star spectrum with noise extraction in V6.0cf (bottom left). Noise estimated with side CDDs V7.0ab (top right). Example of star spectrum with noise extraction in V7.0ab (bottom right). Vertical black bars indicate the various CCDs. The x-axis indicates the CCD column index. 0 to 500 covers the UV part, 248 to 400 nm; 501 to 1400 covers 675 to 400 nm reverse order); then there is the CCD devoted to O₂ band around 760 nm, and the one devoted to H₂O around 936 nm, up to pixel 2338.

[Title Page](#)
[Abstract](#)
[Introduction](#)
[Conclusions](#)
[References](#)
[Tables](#)
[Figures](#)
[⏪](#)
[⏩](#)
[◀](#)
[▶](#)
[Back](#)
[Close](#)
[Full Screen / Esc](#)
[Printer-friendly Version](#)
[Interactive Discussion](#)

**Ozone monitoring
with the
GOMOS-ENVISAT
experiment version 5**

P. Keckhut et al.

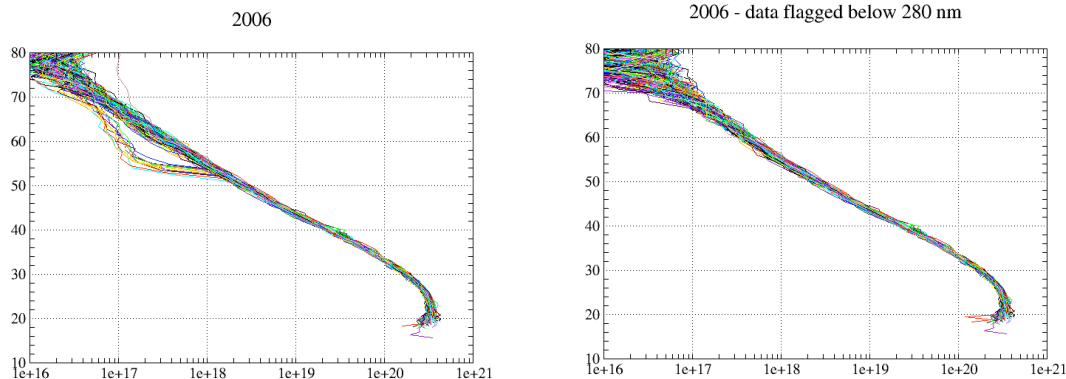


Fig. 3. O₃ line density profiles obtained with a dim star S143 in 2006 using the V6.0cf processing (left panel) and same set of profiles re-calculated removing a part of the spectrum (240–280 nm).

[Title Page](#)[Abstract](#)[Introduction](#)[Conclusions](#)[References](#)[Tables](#)[Figures](#)[⏪](#)[⏩](#)[◀](#)[▶](#)[Back](#)[Close](#)[Full Screen / Esc](#)[Printer-friendly Version](#)[Interactive Discussion](#)

**Ozone monitoring
with the
GOMOS-ENVISAT
experiment version 5**

P. Keckhut et al.

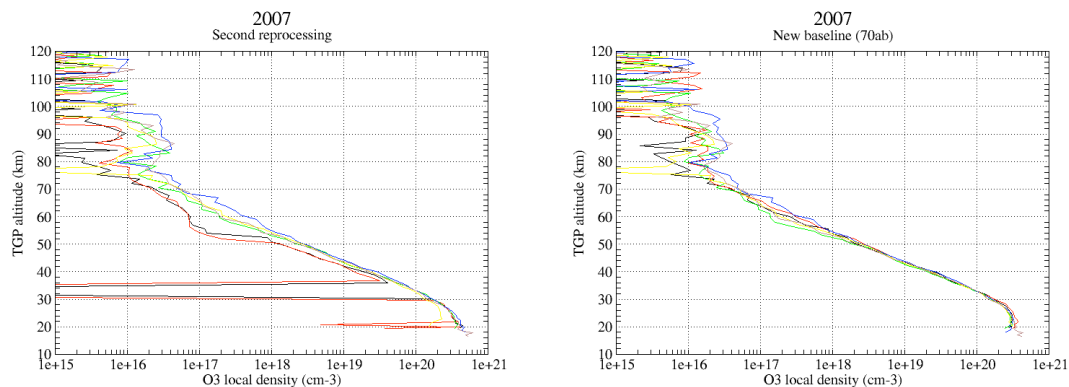


Fig. 4. O₃ line density profiles retrieved from occultations of a dim star S143 in 2007 processed with the V6.0cf algorithm including DSA dark charge estimate (left) and V7.0ab processing including background bands to better estimate the Dark Charge of the central band (right).

[Title Page](#)[Abstract](#)[Introduction](#)[Conclusions](#)[References](#)[Tables](#)[Figures](#)[◀](#)[▶](#)[◀](#)[▶](#)[Back](#)[Close](#)[Full Screen / Esc](#)[Printer-friendly Version](#)[Interactive Discussion](#)

Ozone monitoring with the GOMOS-ENVISAT experiment version 5

P. Keckhut et al.

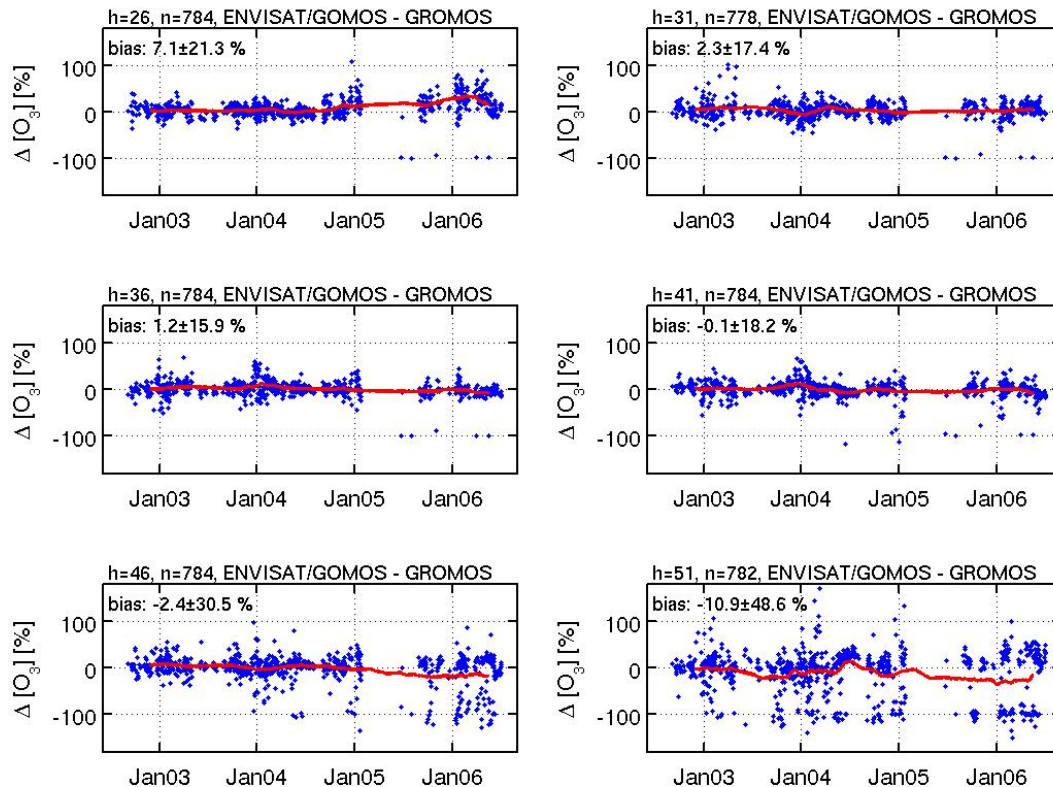


Fig. 5. Time series of the relative difference ΔO_3 of the ozone concentration profiles of ENVISAT/GOMOS and the ground-based microwave radiometer GROMOS at altitudes $h=26$, 31, 36, 41, 46, and 51 km. The red line is a moving average over 80 blue dots. Sometimes ENVISAT/GOMOS fails to detect ozone at upper altitudes (lower panels at $h=46$ and 51 km with ΔO_3 values of about -100%). N corresponds to the number of collocations.

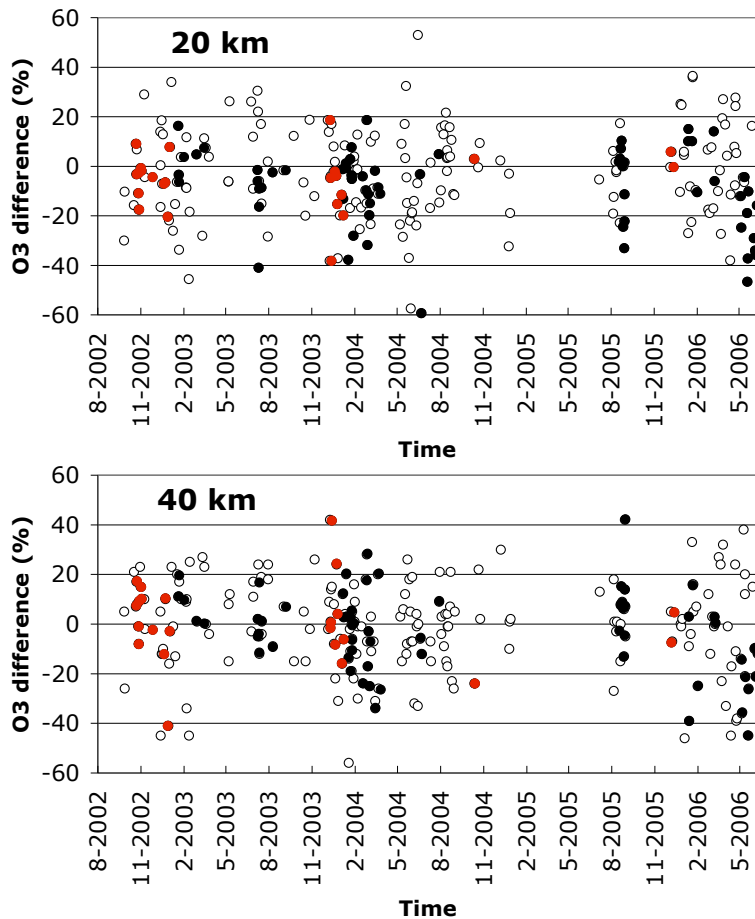


Fig. 6. Data comparison between GOMOS and the OHP DIAL lidar at 20 km (a) and 40 km (b). Black dots correspond to the bright and twilight illumination conditions while the best star spectrum are represented with red dots.

Title Page	
Abstract	Introduction
Conclusions	References
Tables	Figures
◀	▶
◀	▶
Back	Close
Full Screen / Esc	
Printer-friendly Version	
Interactive Discussion	

